DALTON
FULL PAPER

# Synthesis and electrochemistry of $[Ru(2,2'\text{-bpy})_3]_2[S_2Mo_{18}O_{62}]$ at electrode–solvent (electrolyte) interfaces

**Victoria M. Hultgren,[a] Alan M. Bond *[a] and Anthony G. Wedd [b]**

[a] *School of Chemistry, PO Box 23, Monash University, Victoria 3800, Australia. E-mail: a.bond@sci.monash.edu.au; Fax: +61 3 9905 9129*
[b] *School of Chemistry, University of Melbourne, Parkville, Victoria 3010, Australia*

***Received 27th October 2000, Accepted 30th January 2001***
***First published as an Advance Article on the web 8th March 2001***

Addition of $[Ru(bpy)_3][PF_6]_2$ to $[(C_6H_{13})_4N]_4[S_2Mo_{18}O_{62}]$ in $CH_3CN$ resulted in the formation of analytically pure $[Ru(bpy)_3]_2[S_2Mo_{18}O_{62}]$. Insolubility in $CH_3CN$ and solubility in DMF allow solid state and solution phase electrochemical data to be compared. Voltammetric studies of $[Ru(bpy)_3]_2[S_2Mo_{18}O_{62}]$ adhered to a glassy carbon electrode surface and placed in contact with $CH_3CN$ (0.1 M $Bu_4NPF_6$) indicate diffusion of ions within the solid occurs rapidly in order to achieve charge neutralisation required for oxidation of the $[Ru(bpy)_3]^{2+}$ cation and reduction of the $[S_2Mo_{18}O_{62}]^{4-}$ anion. Mass increases on the electrode surface (detected by the electrochemical quartz crystal microbalance method) accompany both oxidation and reduction processes, eqns. (i)–(iv). Cyclic voltammetry

$$[Ru(bpy)_3]_2[S_2Mo_{18}O_{62}]\ (solid) + PF_6^-\ (solution) \underset{+e^-}{\overset{-e^-}{\rightleftharpoons}} [Ru(bpy)_3]_2[S_2Mo_{18}O_{62}][PF_6]\ (solid) \quad (i)$$

$$[Ru(bpy)_3]_2[S_2Mo_{18}O_{62}]\ (solid) + Bu_4N^+\ (solution) \underset{-e^-}{\overset{+e^-}{\rightleftharpoons}} [Bu_4N][Ru(bpy)_3]_2[S_2Mo_{18}O_{62}]\ (solid) \quad (ii)$$

$$[Bu_4N][Ru(bpy)_3]_2[S_2Mo_{18}O_{62}]\ (solid) + Bu_4N^+\ (solution) \underset{-e^-}{\overset{+e^-}{\rightleftharpoons}} [Bu_4N]_2[Ru(bpy)_3]_2[S_2Mo_{18}O_{62}]\ (solid) \quad (iii)$$

$$[Bu_4N]_2[Ru(bpy)_3]_2[S_2Mo_{18}O_{62}]\ (solid) + Bu_4N^+\ (solution) \underset{-e^-}{\overset{+e^-}{\rightleftharpoons}} [Bu_4N]_3[Ru(bpy)_3]_2[S_2Mo_{18}O_{62}]\ (solid) \quad (iv)$$

of 0.2 mM $[Ru(bpy)_3]_2[S_2Mo_{18}O_{62}]$ in DMF (0.1 M $Bu_4NPF_6$) reveals one reversible oxidation ($E^r_{1/2}$ + 791 mV) and two reversible fully solution phase diffusion controlled reduction reactions ($E^r_{1/2}$ −33 and −310 mV *vs.* $Fc^+$/Fc), corresponding to the $[Ru(bpy)_3]^{2+/3+}$ and $[S_2Mo_{18}O_{62}]^{4-/5-}$ and $[S_2Mo_{18}O_{62}]^{5-/6-}$ charge transfer processes, respectively. With 1 mM $[Ru(bpy)_3]_2[S_2Mo_{18}O_{62}]$ in DMF (0.1 M $Bu_4NPF_6$) precipitation on the electrode surface occurs on scanning to potentials more negative than the initial reduction process, due to formation of $[Bu_4N]_2[Ru(bpy)_3]_2$-$[S_2Mo_{18}O_{62}]$. Enhanced levels of surface based processes are also observed in the voltammetry of $[Ru(bpy)_3]_2$-$[S_2Mo_{18}O_{62}]$ in DMF (0.01 M $Bu_4NPF_6$), corresponding to precipitation of $[Bu_4N][Ru(bpy)_3]_2[S_2Mo_{18}O_{62}]$ and $[Ru(bpy)_3]_2[S_2Mo_{18}O_{62}][PF_6]$ on the electrode surface. Data imply that mixed cation salts are more soluble than those containing only $[Ru(bpy)_3]^{2+}$ in all redox levels.

## Introduction

The chemical, photochemical and electrochemical properties of polyoxometalate anions have been of interest in recent years [1] because of their application to catalysis, medicinal chemistry, analytical chemistry and solid state technologies. In the area of electrocatalysis, extensive studies have been undertaken to probe the nature of films of polyoxometalates formed on electrode surfaces in the presence of a range of cations, including $[Os(bpy)_3]^{2+}$ and $[Ru(bpy)_3]^{2+}$ (bpy = 2,2′-bipyridine).[2] In particular, it has been shown by Kuhn and Anson that alternating layers of $[P_2Mo_{18}O_{62}]^{6-}$ and $[Os(bpy)_3]^{2+}$ may be irreversibly adsorbed onto electrode surfaces.[3] These stable redox-active multi-layers are promising for use as electrochromic devices, electron transfer mediators in sensors and for electrocatalytic surfaces. Although no details were provided, it was suggested that analogous $[Ru(bpy)_3]^{2+}$–polyoxometalate films would be accessible, although possible structural limitations may exist.[3]

In order to explore the properties of the ruthenium polyoxometalate materials, we have synthesized $[Ru(bpy)_3]_2[S_2Mo_{18}O_{62}]$ and studied its redox chemistry in both solution and solid phases. The salt is insoluble in all common solvents except dimethylformamide (DMF). Consequently, solution phase data are accessible in DMF (electrolyte) media and studies using solid $[Ru(bpy)_3]_2[S_2Mo_{18}O_{62}]$ attached to an electrode placed in acetonitrile (electrolyte) are possible. Relationships between solution and solid phase redox chemistry can therefore be established.

## Results and discussion

### A Solution phase voltammetry of $[(C_6H_{13})_4N]_4[S_2Mo_{18}O_{62}]$ and $[Ru(bpy)_3]_2[PF_6]_2$ in DMF and $CH_3CN$

A detailed knowledge of the redox processes that occur for $[S_2Mo_{18}O_{62}]^{4-}$ and $[Ru(bpy)_3]^{2+}$ in solution is essential background for the study of the redox chemistry of $[Ru(bpy)_3]_2$-$[S_2Mo_{18}O_{62}]$ and related solids at electrode–solid–solvent (electrolyte) interfaces. The voltammetry of $[S_2Mo_{18}O_{62}]^{4-}$ has been defined in $CH_3CN$ (0.05–0.2 M $Bu_4NClO_4$) [4–6] and reveals an extensive series of eight one electron reversible reduction processes. Four reversible reduction processes were observed for $[S_2Mo_{18}O_{62}]^{4-}$ (1 mM) in DMF (0.1 M $Bu_4NPF_6$) under conditions of cyclic voltammetry at a glassy carbon electrode over the potential range +400 to −1600 mV (Fig. 1a, Table 1). These processes correspond to the solution phase reaction

 DOI: 10.1039/b008682g

**Table 1** Half wave potentials for the reduction of $[S_2Mo_{18}O_{62}]^{4-}$ and oxidation of $[Ru(bpy)_3]^{2+}$ in DMF and $CH_3CN$ (0.1 M $Bu_4NPF_6$) obtained by cyclic voltammetry at a glassy carbon electrode using a scan rate of 100 mV $s^{-1}$

| | $E_{1/2}$ ($[(C_6H_{13})_4N]_4[S_2Mo_{18}O_{62}]$)/mV | | | $E_{1/2}$ ($[Ru(bpy)_3][PF_6]_2$)/mV | |
|---|---|---|---|---|---|
| Process | DMF | $CH_3CN$ | Process | DMF | $CH_3CN$ |
| $[S_2Mo_{18}O_{62}]^{4-/5-}$ | −22 | 100 | $[Ru(bpy)_3]^{3+/2+}$ | +799 | +890 |
| $[S_2Mo_{18}O_{62}]^{5-/6-}$ | −322 | −137 | $[Ru(bpy)_3]^{2+/1+}$ | −1741 | −1721 |
| $[S_2Mo_{18}O_{62}]^{6-/7-}$ | −1026 | −793 | $[Ru(bpy)_3]^{1+/0}$ | −1924 | −1911 |
| $[S_2Mo_{18}O_{62}]^{7-/8-}$ | −1327 | −1069 | $[Ru(bpy)_3]^{0/1-}$ | −2193 | −2159 |

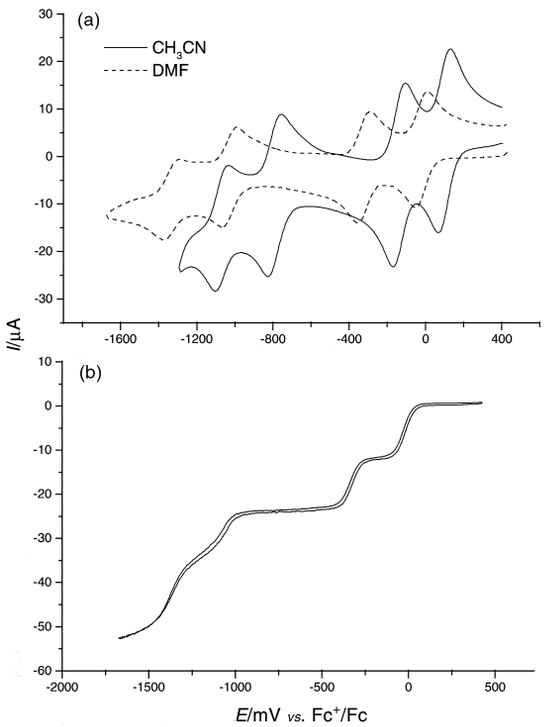


**Fig. 1** Electrochemistry of $[(C_6H_{13})_4N]_4[S_2Mo_{18}O_{62}]$ (1 mM) in the presence of $Bu_4NPF_6$ (0.1 M). (a) Cyclic voltammograms in DMF and $CH_3CN$; $v$ 100 mV $s^{-1}$. (b) Steady state hydrodynamic voltammogram in DMF; $v$ 10 mV $s^{-1}$. Rotation speed 500 rpm.

sequence given in eqn. (1). Reduction processes at more negative

$$[S_2Mo_{18}O_{62}]^{4-} \underset{-e^-}{\overset{+e^-}{\rightleftharpoons}} [S_2Mo_{18}O_{62}]^{5-} \underset{-e^-}{\overset{+e^-}{\rightleftharpoons}} [S_2Mo_{18}O_{62}]^{6-} \underset{-e^-}{\overset{+e^-}{\rightleftharpoons}} [S_2Mo_{18}O_{62}]^{7-} \underset{-e^-}{\overset{+e^-}{\rightleftharpoons}} [S_2Mo_{18}O_{62}]^{8-} \quad (1)$$

potentials were less well defined in DMF than in $CH_3CN$[5] and are not considered further here.

Reversible values of $E^r_{1/2}$ ($E^r_{1/2}$ = half-wave potential calculated as $(E_p^{red} + E_p^{ox})/2$) are shifted cathodically and $\Delta E_p$ values ($E_p^{red}$, $E_p^{ox}$ and $\Delta E_p$ are reduction, oxidation and peak-to-peak potentials, respectively) are larger in DMF relative to those observed in $CH_3CN$. The solvent dependence of $E^r_{1/2}$ values is consistent with DMF having a smaller acceptor number than $CH_3CN$ (16.0 compared with 19.3).[7] Analysis of limiting current values and wave shapes of steady-state hydrodynamic voltammograms (Fig. 1b) at a rotating disk electrode confirmed that each reduction step in DMF was associated with a reversible one electron charge transfer process, as has been found with $CH_3CN$.[4–6] In addition the diffusion coefficient, $D$, calculated from the Randles–Sevcik (cyclic voltammetry) and Levich (rotating disk voltammetry) equations for $[S_2Mo_{18}O_{62}]^{4-}$ in DMF is $2.3 \times 10^{-6}$ $cm^2$ $s^{-1}$, whilst that in $CH_3CN$ is $6.6 \times 10^{-6}$ $cm^2$ $s^{-1}$. This smaller $D$ value in DMF is reflected by smaller current responses per unit $[S_2Mo_{18}O_{62}]^{4-}$ concentration for the reduction processes in this solvent.

A solution of $[Ru(bpy)_3]^{2+}$ (1 mM) in DMF or $CH_3CN$ (0.1 M $Bu_4NPF_6$) gave the expected $Ru^{3+/2+}$ metal-based redox process (eqn. 2) and three bipyridine ligand reduction processes

$$[Ru(bpy)_3]^{2+} \underset{+e^-}{\overset{-e^-}{\rightleftharpoons}} [Ru(bpy)_3]^{3+} \quad (2)$$

(eqn. 3). Observed $E^r_{1/2}$ values (Table 1) agree with those reported previously.[8]

$$[Ru(bpy)_3]^{2+} \underset{-e^-}{\overset{+e^-}{\rightleftharpoons}} [Ru(bpy)_3]^{+} \underset{-e^-}{\overset{+e^-}{\rightleftharpoons}} [Ru(bpy)_3]^{0} \underset{-e^-}{\overset{+e^-}{\rightleftharpoons}} [Ru(bpy)_3]^{-} \quad (3)$$

Examination of data in Table 1 suggests that the processes summarised in eqns. (1) and (2) would be fully resolved for the salt $[Ru(bpy)_3]_2[S_2Mo_{18}O_{62}]$, but that a complex overlap of processes summarised in eqn. (3) and those for $[S_2Mo_{18}O_{62}]^{8-/9-}$, $^{9-/10-}$, *etc.* at very negative potentials would occur. Consequently, we have not examined the very negative potential region in studies on $[Ru(bpy)_3]_2[S_2Mo_{18}O_{62}]$.

### B Voltammetry of $[Ru(bpy)_3]_2[S_2Mo_{18}O_{62}]$ in DMF

$[Ru(bpy)_3]_2[S_2Mo_{18}O_{62}]$ is only sparingly soluble in DMF. The solubility product, $K_{sp}$, is estimated to be about $4 \times 10^{-11}$ $M^3$ $L^{-3}$. However, the solid is significantly more soluble in the presence of added $Bu_4NPF_6$ presumably due to the enhanced solubility of $Bu_4N^+$ salts. Consequently, the role of the electrolyte is significant and voltammetric studies on DMF solutions of $[Ru(bpy)_3]_2[S_2Mo_{18}O_{62}]$ containing 0.1 and 0.01 M $Bu_4NPF_6$ are reported.

**(i) In the presence of 0.1 M $Bu_4NPF_6$.** Analysis of voltammograms established a well defined reversible one electron oxidation process corresponding to the $[Ru(bpy)_3]^{2+/3+}$ couple (eqn. 2; Fig. 2a). The $E_{1/2}$ value of +808 mV is close to that obtained in the absence of $[S_2Mo_{18}O_{62}]^{4-}$. However, only the initial reduction step had the characteristics of a reversible one electron diffusion controlled process (Fig. 2b and 2c). This was followed by a series of processes indicating interaction with the surface, rather than the series of well defined diffusion controlled processes observed separately for $[(C_6H_{13})_4N]_4[S_2Mo_{18}O_{62}]$ and $[Ru(bpy)_3][PF_6]_2$ under the same conditions (eqns. (1) and (3)).

The first diffusion controlled reduction process in DMF (0.1 M $Bu_4NPF_6$) (Fig. 2b and 2c) has an $E_{1/2}$ value of −6 mV, which is 17 mV more positive than found for $[(C_6H_{13})_4N]_4[S_2Mo_{18}O_{62}]$ under the same conditions. This is therefore assigned to reaction (4), with the $[Ru(bpy)_3]^{2+}$ cation playing a minor role

$$[S_2Mo_{18}O_{62}]^{4-} \text{ (solution)} + e^- \rightleftharpoons [S_2Mo_{18}O_{62}]^{5-} \text{ (solution)} \quad (4)$$

only, presumably *via* ion pairing. However, clearly the presence of the $[Ru(bpy)_3]^{2+}$ cation modifies the subsequent $[S_2Mo_{18}O_{62}]^{4-}$ reduction processes in a fundamentally more significant manner than expected from ion-pair considerations alone. A

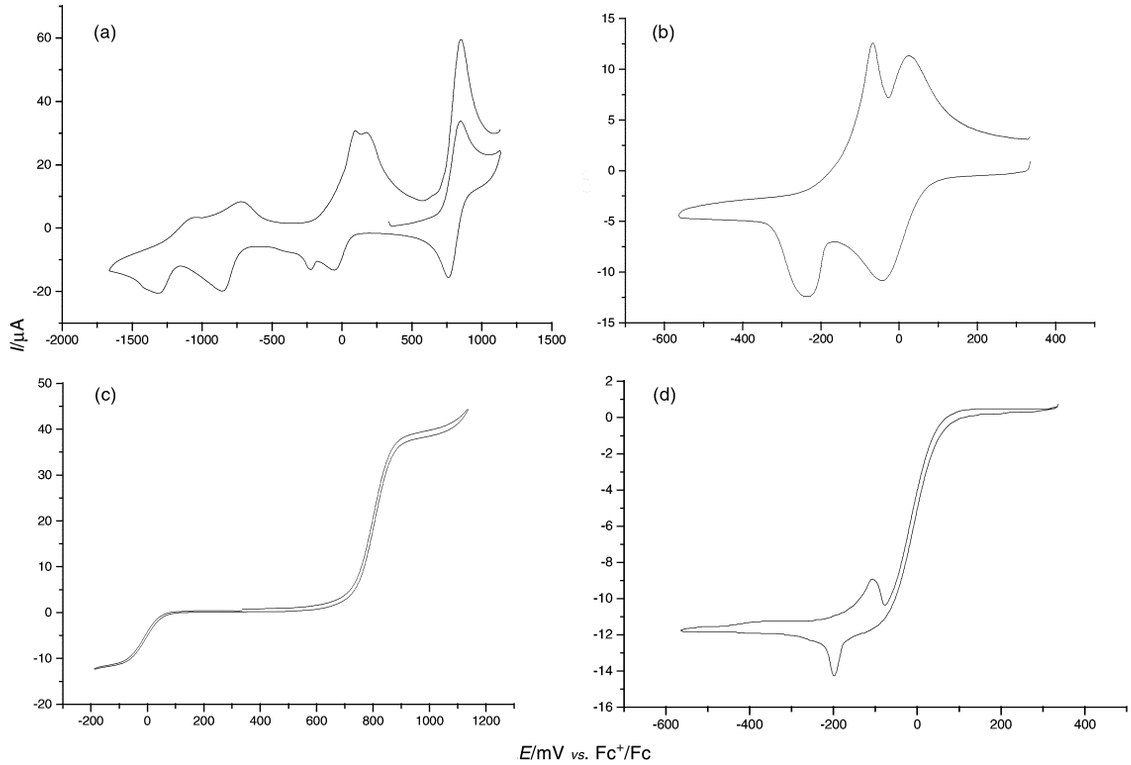


**Fig. 2** Electrochemistry of $[Ru(bpy)_3]_2[S_2Mo_{18}O_{62}]$ (1 mM) in DMF (0.1 M $Bu_4NPF_6$). (a) and (b) Cyclic voltammetry with different initial and switching potentials; $v$ 100 mV $s^{-1}$. (c) and (d) Hydrodynamic voltammetry over different potential ranges; $v$ 10 mV $s^{-1}$, rotation speed 500 rpm.

rotating disk voltammogram (Fig. 2d) reveals that the second $[S_2Mo_{18}O_{62}]^{4-}$ reduction process is barely detectable in the presence of $[Ru(bpy)_3]^{2+}$ and clearly is not mass transport controlled.

The first solution phase and second reduction processes were studied at a number of different rotation speeds and scan rates. It was found that increasing either the scan rate or the rotation speed did not eliminate the occurrence of the surface based features associated with the second and subsequent reduction processes. The interpretation proposed to explain the voltammetry is that precipitation of a mixed cation solid such as $[Bu_4N]_2[Ru(bpy)_3]_2[S_2Mo_{18}O_{62}]$ is extremely rapid and occurs once reduction of dissolved $[S_2Mo_{18}O_{62}]^{5-}$ commences. The proposed reaction pathway for formation of this material is given in eqn. (5).

$$[S_2Mo_{18}O_{62}]^{5-}\ (\text{solution}) \underset{-e^-}{\overset{+e^-}{\rightleftharpoons}} [S_2Mo_{18}O_{62}]^{6-}\ (\text{solution})$$
$$\xrightarrow[[Ru(bpy)_3]^{2+},\ Bu_4N^+]{\text{fast}} [Bu_4N]_2[Ru(bpy)_3]_2[S_2Mo_{18}O_{62}]\ (\text{solid}) \quad (5)$$

**(ii) In the presence of 0.01 M $Bu_4NPF_6$.** A saturated solution (≈0.2 mM) could be prepared from $[Ru(bpy)_3][PF_6]_2$ (2 mM) and $[(C_6H_{13})_4N]_4[S_2Mo_{18}O_{62}]$ (1 mM) (or the dissolution of $[Ru(bpy)_3]_2[S_2Mo_{18}O_{62}]$ by sonication of the equivalent mass of solid for 30 min). The voltammetry shows that both the $[S_2Mo_{18}O_{62}]^{4-/5-}$ and $[S_2Mo_{18}O_{62}]^{5-/6-}$ reduction processes are significantly modified by the presence of $[Ru(bpy)_3]^{2+}$ (Fig. 3) and also that distinct differences exist relative to the equivalent processes with 0.1 M $Bu_4NPF_6$ electrolyte. In particular, both the $[S_2Mo_{18}O_{62}]^{5-}$ and $[Ru(bpy)_3]^{3+}$ species now appear to be surface active and apparently precipitate onto the electrode surface. The influence of uncompensated resistance (IR drop) is also significant when the electrolyte concentration is only 0.01 M.†

The voltammetric data suggest that pure $[Ru(bpy)_3]_2[S_2Mo_{18}O_{62}]$, $[Ru(bpy)_3]_5[S_2Mo_{18}O_{62}]_2$ and $[Ru(bpy)_3]_3[S_2Mo_{18}O_{62}]$ salts are more insoluble than mixed cation salts such as $[Bu_4N]_2[Ru(bpy)_3][S_2Mo_{18}O_{62}]$, $[Bu_4N][Ru(bpy)_3]_2[S_2Mo_{18}O_{62}]$ and $[Bu_4N]_2[Ru(bpy)_3]_2[S_2Mo_{18}O_{62}]$ and that oxidised and reduced forms of the complexes are less soluble than $[Ru(bpy)_3]_2[S_2Mo_{18}O_{62}]$. Thus, lowering the electrolyte concentration favours precipitation of solid after oxidation and reduction. It can also be implied that $[Bu_4N]_2[Ru(bpy)_3][S_2Mo_{18}O_{62}]$ is more soluble than $[Ru(bpy)_3]_2[S_2Mo_{18}O_{62}]$ by the fact that the latter salt is more soluble in DMF in the presence of a large excess of $Bu_4N^+$ and by noting that lowering the electrolyte concentration leads to a decrease in the concentration of dissolved $[Ru(bpy)_3]_2[S_2Mo_{18}O_{62}]$. In accordance with these considerations it was found that the voltammetry of $[Ru(bpy)_3]_2[S_2Mo_{18}O_{62}]$ (0.2 mM) in DMF (0.1 M $Bu_4NPF_6$) reveals both a solution phase diffusion controlled reversible oxidation process ($E_{1/2}$ +791 mV) and two solution phase diffusion controlled reversible, well defined reduction processes ($E_{1/2}$ −33 and −310 mV) without any evidence of precipitation or solid state reactions, in contrast to studies with 1 mM $[Ru(bpy)_3]_2[S_2Mo_{18}O_{62}]$. We can conclude from this information that $[Bu_4N][Ru(bpy)_3]_2[S_2Mo_{18}O_{62}]$ and $[Bu_4N]_2[Ru(bpy)_3]_2[S_2Mo_{18}O_{62}]$ have a restricted level of solubility in DMF (0.1 M $Bu_4NPF_6$), beyond which they are rapidly precipitated onto the electrode surface.

## C Electrochemical quartz crystal microbalance (EQCM) studies in DMF

The voltammetric data implied that precipitation (or adsorption) of solid material occurs during the course of voltammetric experiments on $[Ru(bpy)_3]_2[S_2Mo_{18}O_{62}]$ dissolved in DMF (0.1 or 0.01 M $Bu_4NPF_6$). Microgravimetric EQCM measurements were used to interrogate the nature of the surface based processes.

**(i) In the presence of 0.1 M $Bu_4NPF_6$.** EQCM experiments at a gold electrode with solutions containing either $[Ru(bpy)_3][PF_6]_2$ (2 mM) and $[(C_6H_{13})_4N]_4[S_2Mo_{18}O_{62}]$ (1 mM) in DMF

† The voltammetry of $[(C_6H_{13})_4N]_4[S_2Mo_{18}O_{62}]$ and $[Ru(bpy)_3[PF_6]_2$ in DMF are not significantly altered when the electrolyte concentration is reduced from 0.1 to 0.01 M.

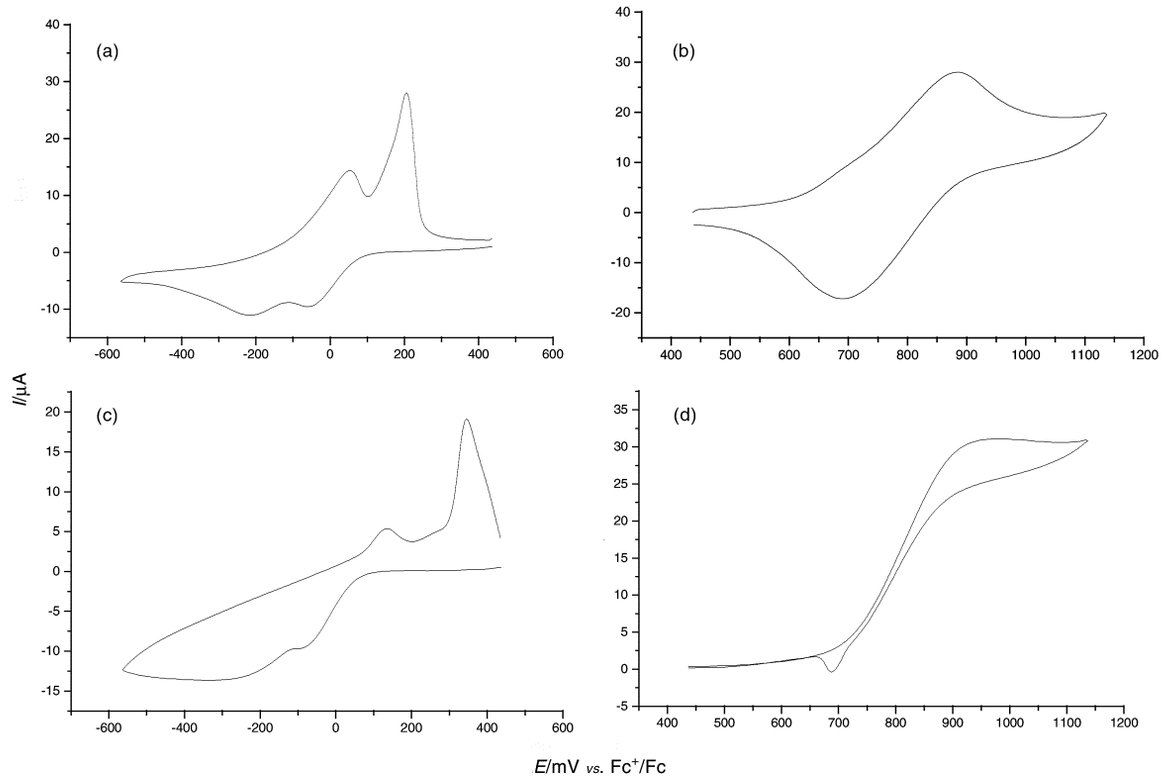


**Fig. 3** Voltammetry of $[Ru(bpy)_3]_2[S_2Mo_{18}O_{62}]$ (≈0.2 mM) in DMF (0.01 M $Bu_4NPF_6$) at a 3.0 mm diameter glassy carbon electrode. Cyclic voltammograms for (a) reduction of $[S_2Mo_{18}O_{62}]^{4-}$ and (b) oxidation of $[Ru(bpy)_3]^{2+}$; *v* 100 mV $s^{-1}$. Hydrodynamic voltammograms over the potential range encompassing (c) the $[S_2Mo_{18}O_{62}]^{4-/5-}$ and $[S_2Mo_{18}O_{62}]^{5-/6-}$ processes and (d) the $[Ru(bpy)_3]^{2+/3+}$ process; *v* 10 mV $s^{-1}$, rotation speed 500 rpm.

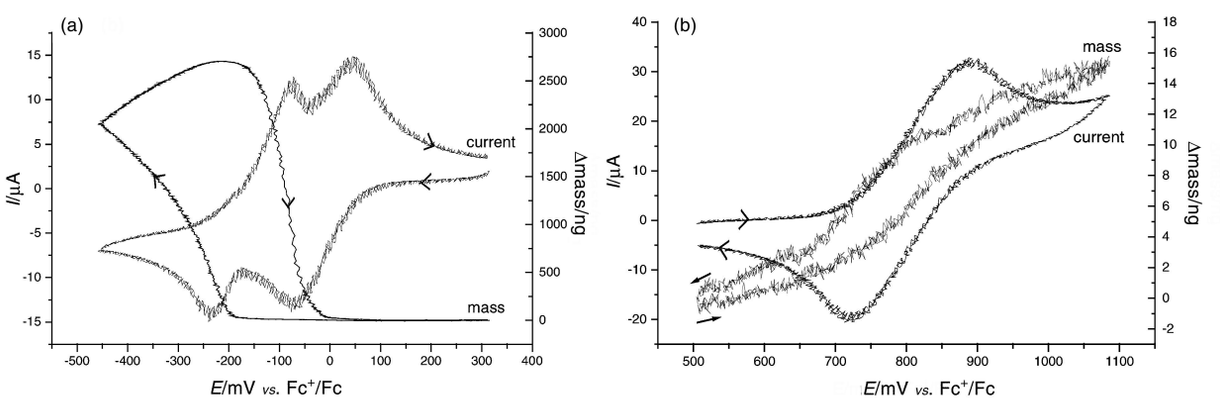


**Fig. 4** The change in mass on a gold electrode surface for a solution containing $[Ru(bpy)_3][PF_6]_2$ (2 mM) and $[(C_6H_{13})_4N]_4[S_2Mo_{18}O_{62}]$ (1 mM) in DMF (0.1 M $Bu_4NPF_6$); *v* 20 mV $s^{-1}$; (a) reduction of $[S_2Mo_{18}O_{62}]^{4-}$, (b) oxidation of $[Ru(bpy)_3]^{2+}$.

(0.1 M $Bu_4NPF_6$) (or the equivalent amount of $[Ru(bpy)_3]_2[S_2Mo_{18}O_{62}]$) revealed that a negligible mass increase accompanied the $[S_2Mo_{18}O_{62}]^{4-/5-}$ process (Fig. 4a). Thus the process remains diffusion controlled even when $[Ru(bpy)_3]^{2+}$ is present as the cation. However, at potentials more negative than −200 mV, which coincides with the onset of the $[S_2Mo_{18}O_{62}]^{5-/6-}$ process, μg quantities of solid rapidly became detected at the gold electrode surface (Fig. 4a).‡ The maximum mass increase is consistent with electrode adsorption of many layers of solid or more likely precipitated two electron reduced material being present on the electrode surface. However, the adhered solid does not lead to electrode blockage so that ion transport must be able to occur within the solid, presumably *via* a layered structure. The mass continued to increase even after the potential was switched at −450 mV and attained a maximum value on the reverse scan at −200 mV under the conditions of Fig. 4a. On the reverse scan at potentials more positive than −200 mV (coinciding with the onset of oxidation of $[S_2Mo_{18}O_{62}]^{6-}$ back to $[S_2Mo_{18}O_{62}]^{5-}$) the mass of solid on the electrode surface decreased rapidly until the potential reached 0 mV. All mass attached to the electrode during the course of reduction was removed once the potential had returned to the initial value of +300 mV.

A barely detectable mass change in the ng region was detected on the electrode surface when the potential was scanned from +500 to +1100 mV (Fig. 4b), as expected if the voltammetry of the $[Ru(bpy)_3]^{2+/3+}$ process remains essentially diffusion controlled even in the presence of $[S_2Mo_{18}O_{62}]^{4-}$.

**(ii) In the presence of 0.01 M $Bu_4NPF_6$.** An equivalent EQCM experiment with lower electrolyte concentration reveals a greater increase in mass upon the electrode on scanning the potential from +500 to −550 mV (Fig. 5a). A larger potential window was scanned than in the previous experiment due

‡ Altering the electrode surface from glassy carbon to Au results in only minor differences in the voltammetric response.

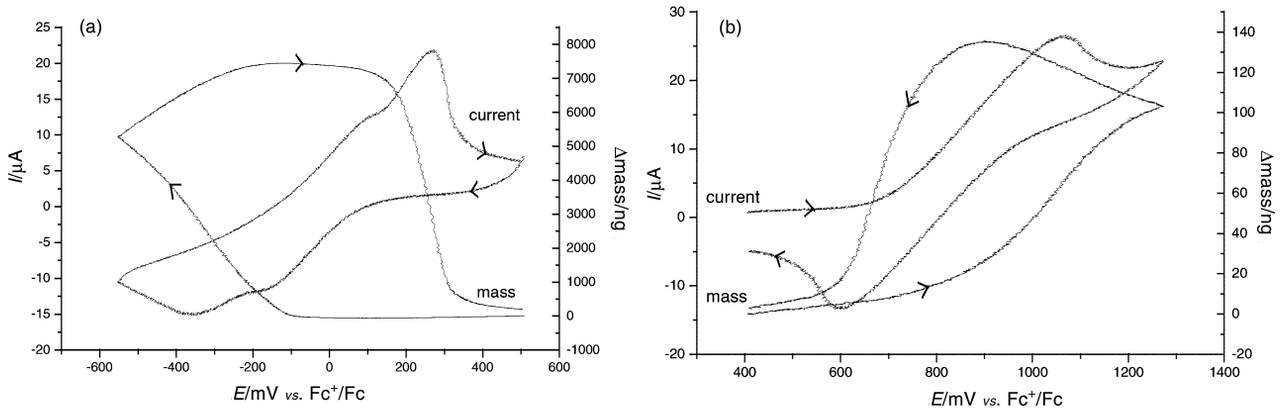


**Fig. 5** The change in mass on a gold electrode surface for a solution containing $[Ru(bpy)_3][PF_6]_2$ (2 mM) and $[(C_6H_{13})_4N]_4[S_2Mo_{18}O_{62}]$ (1 mM) in DMF (0.01 M $Bu_4NPF_6$); $\nu$ 20 mV $s^{-1}$; (a) reduction of $[S_2Mo_{18}O_{62}]^{4-}$, (b) oxidation of $[Ru(bpy)_3]^{2+}$.

to the enhanced IR drop (low electrolyte concentration) giving rise to significant broadening of the voltammetric responses. Under these low electrolyte concentration conditions a small but readily detected mass increase also accompanies the $[S_2Mo_{18}O_{62}]^{4-/5-}$ process. At −100 mV (onset of the $[S_2Mo_{18}O_{62}]^{5-/6-}$ process) the mass on the electrode surface starts to increase rapidly and continues to do so until the potential is switched at about −550 mV. After switching the potential scan direction the mass on the electrode surface increases further, reaching a maximum value at about −200 mV. There is a very small decrease in mass on the electrode surface between −200 and +100 mV on the reverse scan. At potentials more positive than +100 mV the mass on the electrode surface decreases rapidly (during reoxidation of $[S_2Mo_{18}O_{62}]^{5-}$ to $[S_2Mo_{18}O_{62}]^{4-}$) but never quite returning to zero, even when a potential of about +500 mV has been reached, indicating that some material has been left on the electrode surface after one complete cycle of the potential.

Under the low electrolyte concentration conditions significant mass changes now also accompany the $[Ru(bpy)_3]^{2+/3+}$ oxidation process. A small mass increase on the electrode surface is observed on scanning between +400 and +1300 mV (Fig. 5b). On switching the potential at +1300 mV the mass continues to increase, reaching a maximum at +900 mV. The mass decreases on scanning more negative than +900 mV, but never returns to zero, indicating again that some solid material has been left on the electrode surface.

These EQCM experiments confirm that the surface based processes, resulting from the oxidation or reduction of dissolved $[Ru(bpy)_3]_2[S_2Mo_{18}O_{62}]$, markedly depend on the concentration of supporting electrolyte in solution. Surface based precipitates giving thick films or microcrystals having structures enabling rapid transport of ions within the solid are indicated to be formed and the presence of electrolyte can clearly influence the composition of the solid adhered to the electrode surface.

### D Solid state voltammetry of $[Ru(bpy)_3]_2[S_2Mo_{18}O_{62}]$

$[Ru(bpy)_3]_2[S_2Mo_{18}O_{62}]$ can be attached to an electrode surface as a finely ground solid and its voltammetry and redox interconversion studied when the electrode is placed in $CH_3CN$ (0.1 M $Bu_4NPF_6$), provided ion transport can be achieved across the solvent–solid interface to achieve charge neutralisation.

Voltammograms of solid $[Ru(bpy)_3]_2[S_2Mo_{18}O_{62}]$ attached to a glassy carbon electrode surface immersed in $CH_3CN$ (0.1 M $Bu_4NPF_6$) are shown in Fig. 6 at a scan rate of 100 mV $s^{-1}$. The solid state $[Ru(bpy)_3]^{2+/3+}$ oxidation process is well defined (Fig. 6a), with an $E_{1/2}$ value of +895 mV, 5 mV more positive than that observed for the free $[Ru(bpy)_3]^{2+}$ ion in solution (Table 1). The process is summarised in eqn. (6).

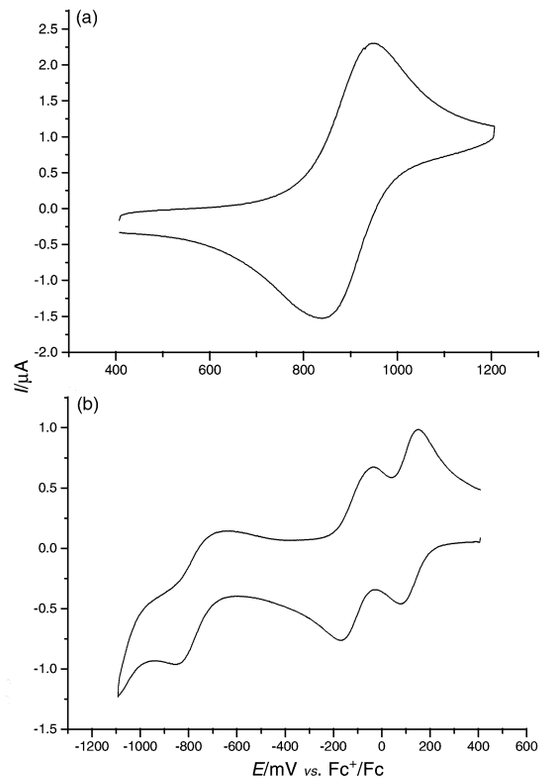


**Fig. 6** Voltammetry of solid $[Ru(bpy)_3]_2[S_2Mo_{18}O_{62}]$ adhered to a glassy carbon electrode surface and immersed in $CH_3CN$ (0.1 M $Bu_4NPF_6$); $\nu$ 100 mV $s^{-1}$; (a) oxidation of $[Ru(bpy)_3]^{2+}$, (b) reduction of $[S_2Mo_{18}O_{62}]^{4-}$.

$$[Ru(bpy)_3]_2[S_2Mo_{18}O_{62}]\ (solid) + PF_6^-\ (solution) \rightleftharpoons [Ru(bpy)_3]_2[S_2Mo_{18}O_{62}][PF_6]\ (solid) + e^- \quad (6)$$

The solid state response is independent of whether or not the solution is stirred so that mass transport of solution phase ions is not indicated. This behaviour is characteristic of diffusion control of ions within the solid, as has been observed in the voltammetry of osmium bis(bipyridyl)tetrazine chloride attached to platinum surfaces[9] and also in studies with conducting polymers.[10] SEM images show that the adhered solid material exists as discrete particles on a solid surface, with the solid array probably being many layers thick (Fig. 7).

Three reduction processes were observed over the potential range +500 to −1000 mV (Fig. 6b), with $E_{1/2}$ values of +116, −101 and −744 mV. These values are slightly more positive than those observed for free $[S_2Mo_{18}O_{62}]^{4-}$ in solution (Table 1). The reduction processes are represented in eqns. (7)–(9).

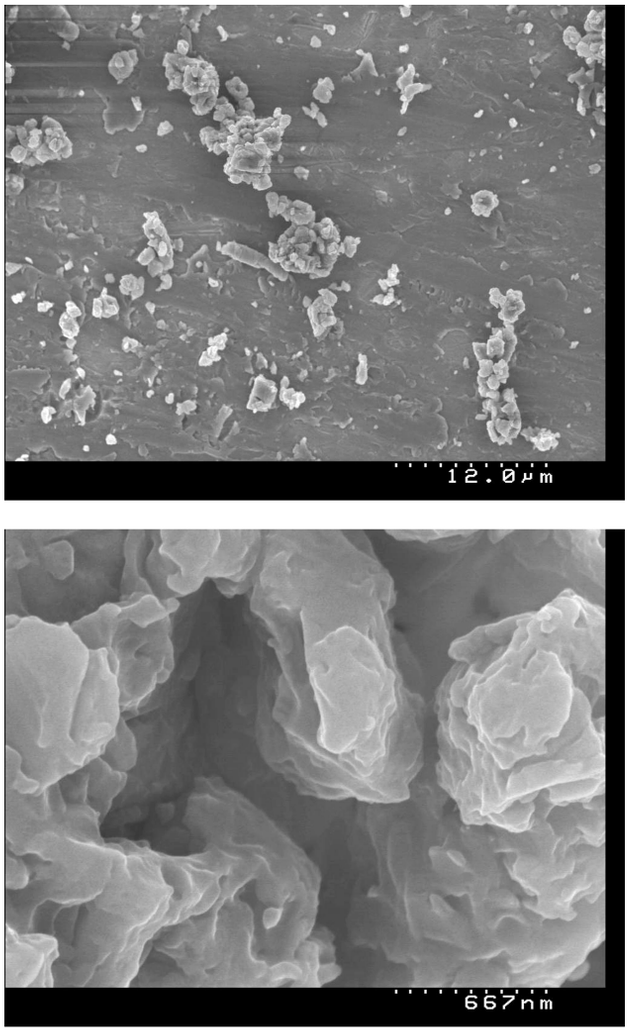


**Fig. 7** Scanning electron microscopy images of $[Ru(bpy)_3]_2[S_2Mo_{18}O_{62}]$ adhered to a brass plate.

$$[Ru(bpy)_3]_2[S_2Mo_{18}O_{62}]\ (solid) + Bu_4N^+\ (solution) \underset{-e^-}{\overset{+e^-}{\rightleftharpoons}} [Bu_4N]_3[Ru(bpy)_3]_2[S_2Mo_{18}O_{62}]\ (solid) \quad (7)$$

$$[Bu_4N][Ru(bpy)_3]_2[S_2Mo_{18}O_{62}]\ (solid) + Bu_4N^+\ (solution) \underset{-e^-}{\overset{+e^-}{\rightleftharpoons}} [Bu_4N]_2[Ru(bpy)_3]_2[S_2Mo_{18}O_{62}]\ (solid) \quad (8)$$

$$[Bu_4N]_2[Ru(bpy)_3]_2[S_2Mo_{18}O_{62}]\ (solid) + Bu_4N^+\ (solution) \underset{-e^-}{\overset{+e^-}{\rightleftharpoons}} [Bu_4N][Ru(bpy)_3]_2[S_2Mo_{18}O_{62}]\ (solid) \quad (9)$$

Scanning to potentials more negative than −1000 mV resulted in the observation of more complex reduction processes.

The uptake of ions required for charge neutralisation (as described in eqns. (7)–(9)) should result in a mass increase on the electrode surface. EQCM experiments on solid $[Ru(bpy)_3]_2[S_2Mo_{18}O_{62}]$ adhered to a gold electrode in contact with $CH_3CN$ (0.1 M $Bu_4NPF_6$) confirm that this is the case for both the oxidation and reduction processes. The fact that solution phase and solid state processes have similar potentials and wave shapes, even though the mass transport processes are significantly different, implies very little interaction of the cation and anion in either the solid state or solution phases. A very open layered solid state structure may be present in $[Ru(bpy)_3]_2[S_2Mo_{18}O_{62}]$ which enables ready penetration of solvent and electrolyte.

## Conclusion

The isolation of $[Ru(bpy)_3]_2[S_2Mo_{18}O_{62}]$ has led us to observe clearly defined, reversible solid state redox processes for both oxidation of the cation and reduction of the anion when the solid is confined to an electrode surface placed in contact with $CH_3CN$ (0.1 M $Bu_4NPF_6$). Counter ions required for charge neutralisation during the course of the oxidation and reduction processes are easily transported between the solution (electrolyte) and solid phases and also within the solid. Mass increases on a gold quartz crystal for the oxidation ($PF_6^-$ uptake) and reduction ($Bu_4N^+$ uptake) processes confirm this to be the case. Thin films of electroactive $[Ru(bpy)_3]_2[S_2Mo_{18}O_{62}]$ on the electrode surface have not been detected by immersing the electrode into a DMF solution containing dissolved compound unlike, for example, $[P_2Mo_{18}O_{62}]^{6-}$ which can readily form monolayer films.[3] Multilayer films also can be achieved by dipping the modified $[P_2Mo_{18}O_{62}]^{6-}$ electrode into a solution containing $[Ru(bpy)_3]^{2+}$ or $[Os(bpy)_3]^{2+}$ cations. However, whilst well defined reduction processes are observed with these multi-layer films, the $[Ru(bpy)_3]^{2+/3+}$ oxidation processes is not observed and the $[Os(bpy)_3]^{2+/3+}$ redox process is only detected when the cation is the last coating on the electrode. Direct attachment of $[Ru(bpy)_3]_2[S_2Mo_{18}O_{62}]$ presumably gives rise to a thick layer of solid that allows ready access of solvent and electrolyte, so that voltammetry of the cation and anion are equally well defined in both the solid state and solution phase processes.

EQCM and cyclic voltammetric studies in DMF (0.1 M $Bu_4NPF_6$) with 1 mM $[Ru(bpy)_3]_2[S_2Mo_{18}O_{62}]$ reveal that the $[S_2Mo_{18}O_{62}]^{5-/6-}$ process is changed from a solution phase to a surface based process by the presence of $[Ru(bpy)_3]^{2+}$, but only minor changes are detected for the $[S_2Mo_{18}O_{62}]^{4-/5-}$ and $[Ru(bpy)_3]^{2+}$ processes. The magnitude of the mass attached to the electrode surface during the course of the $[S_2Mo_{18}O_{62}]^{5-/6-}$ process is far greater than expected for a monolayer thin film coverage and multilayer precipitation is believed to occur. This precipitate formed after the two electron reduction stage is most likely to be a mixed cation salt with the probable stochiometry $[Bu_4N]_2[Ru(bpy)_3]_2[S_2Mo_{18}O_{62}]$. Use of 0.2 mM solutions of $[Ru(bpy)_3]_2[S_2Mo_{18}O_{62}]$ give almost exclusively solution based voltammetry indicating that the solubility of $[S_2Mo_{18}O_{62}]^{6-}$ is electrolyte concentration dependent.

The solubility of $[Ru(bpy)_3]_2[S_2Mo_{18}O_{62}]$ in DMF is also dependent on the concentration of $Bu_4NPF_6$. Lowering the concentration of $Bu_4NPF_6$ to 0.01 M reduces the solubility of $[Ru(bpy)_3]_2[S_2Mo_{18}O_{62}]$ to about 0.2 mM. At these lower concentrations the $[S_2Mo_{18}O_{62}]^{4-/5-}$ reduction and $[Ru(bpy)_3]^{2+/3+}$ oxidation processes also become surface based. EQCM studies confirm mass increases occur on the electrode surface for these processes, with the mass increase being much greater than that observed for $[Ru(bpy)_3]_2[S_2Mo_{18}O_{62}]$ (1 mM) in DMF (0.1 M $Bu_4NPF_6$). It is concluded from these data that as long as the solubility of $[Ru(bpy)_3]_2[S_2Mo_{18}O_{62}]$ and its reduced forms is not exceeded the $[Ru(bpy)_3]^{2+/3+}$, $[S_2Mo_{18}O_{62}]^{4-/5-}$ and $[S_2Mo_{18}O_{62}]^{5-/6-}$ processes are reversible and diffusion controlled and occur in the solution phase.

## Experimental

### Reagents

Acetonitrile ($CH_3CN$; Mallinckrodt, Biolab Scientific, HPLC grade, 99.9%) and dimethylformamide (DMF; Mallinckrodt, Biolab Scientific, HPLC grade, 99.9%) were dried over molecular sieves prior to use. Diethyl ether was used as supplied by Merck. Tetrabutylammonium hexafluorophosphate ($Bu_4NPF_6$) was synthesized as described in reference 11 and used as the supporting electrolyte in all experiments. Ferrocene was used as supplied by BDH chemicals. The synthesis of $[(C_6H_{13})_4N]_4[S_2Mo_{18}O_{62}]$ is described in reference 12. $[Ru(bpy)_3][PF_6]_2$

was kindly donated by Professor G. B. Deacon. All experiments were conducted under ambient temperature conditions (22 ± 1 °C).

### Synthesis of $[Ru(bpy)_3]_2[S_2Mo_{18}O_{62}]$

$[Ru(bpy)_3][PF_6]_2$ (61.4 mg; $7.14 \times 10^{-5}$ mol) in $CH_3CN$ (15 ml) was added with stirring to a solution of $[(C_6H_{13})_4N]_4[S_2Mo_{18}O_{62}]$ (150 mg; $3.57 \times 10^{-5}$ mol) in $CH_3CN$ (20 ml). The resulting dark orange-brown precipitate was stirred for 10 min and then left standing in the dark for 1 h. After this time the solid was filtered off, washed with copious amounts of $CH_3CN$, diethyl ether and dried in the dark in a desiccator (129 mg; 93%). Found: C, 18.58; H, 1.29; N, 3.75; S, 1.61. $C_{30}H_{24}Mo_9N_6O_{31}RuS$ requires: C, 18.49; H, 1.24; N, 3.70; S, 1.65%.

The solubility, $S$, and solubility product, $K_{sp}$, of $[Ru(bpy)_3]_2[S_2Mo_{18}O_{62}]$ in DMF were determined by weighing out a known quantity into 20 ml of the solvent. The mixture was stirred for 1 h and filtered through a glass sinter of known weight. The sinter was dried to constant weight and the mass of $[Ru(bpy)_3]_2[S_2Mo_{18}O_{62}]$ present in a saturated solution of dissolved material in DMF was determined by difference.

### Instrumentation and procedures

Solution phase voltammetric experiments using stationary macro-disk electrodes were carried out in a standard three-electrode arrangement with a glassy carbon disk (0.071 $cm^2$) as the working electrode, a platinum wire as the counter electrode and a $Ag/Ag^+$ ($CH_3CN$, 10 mM $AgNO_3$) double junction reference electrode. The effective electrode area of 0.071 $cm^2$ was determined by measurement of the peak current value obtained for reversible one electron oxidation of a 1 mM solution of ferrocene by cyclic voltammetry and the Randles–Sevcik equation $I_p = (2.69 \times 10^{-5})n^{3/2}AD^{1/2}Cv^{1/2}$ where $I_p$ is the peak current (A), $n$ the number of electrons, $A$ the electrode area ($cm^2$), $D$ the diffusion coefficient (taken to be $2.3 \times 10^{-5}$ $cm^2$ $s^{-1}$ [13]), $C$ the concentration (mol $cm^{-3}$) and $v$ the scan rate (V $s^{-1}$). Electrode potentials are quoted relative to the ferrocenium–ferrocene redox couple ($Fc^+/Fc$) except where otherwise noted. Rotating disk electrode experiments used the same configuration as for stationary solution ones except that the glassy carbon disk working electrode was rotated by a variable speed rotator (Metrohm 628–10). Voltammetric experiments on solids attached to the electrode surface used the same configuration as for the solution experiments except that the glassy carbon working electrode had an effective area of 0.00985 $cm^2$. The relevant solid material was finely ground and mechanically attached to the electrode surface by transfer from solid attached to a cotton bud. The electrode was then immersed into the electrochemical cell containing $CH_3CN$ and $Bu_4NPF_6$ (0.1 M).

A BAS100 (Bioanalytical Systems) Electrochemical System was used in the macro-disk electrode solution phase voltammetric experiments. Solid state electrochemical experiments were carried out on a Cypress Systems (model CYSY-1R) computer controlled electroanalysis system. Electrochemical quartz crystal microbalance experiments were carried out on an ELCHEMA-701 instrument (Postdam, New York) in conjunction with an ELCHEMA PS-205 potentiostat and Voltscan software (Intellect Software, Postdam, New York). 10 MHz AT-cut gold sputtered quartz crystals were purchased from Bright Star Crystals (Vermont, Vic., Australia). The diameter of the gold sputtered area was 5 mm. The quartz crystal was mounted onto the side of a glass cell and held in place by two O-rings.

Scanning electron microscopy (SEM) images of $[Ru(bpy)_3]_2[S_2Mo_{18}O_{62}]$ were obtained with a Hitachi S-5000 system. Solid $[Ru(bpy)_3]_2[S_2Mo_{18}O_{62}]$ was finely ground in the same manner as that attached to electrode surfaces and applied to a polished brass plate using a cotton bud in order to obtain an image.

Oxygen was removed from the solutions by purging with nitrogen. All experiments were carried out in the dark to avoid photochemical reactions reported elsewhere.[14] Microanalyses were carried out by Chemical and Micro Analysis Services Pty. Ltd., Belmont, Victoria, Australia.

## Acknowledgements

We thank A. van den Bergen for supplying the electrolyte, M. Wujian for assistance with the EQCM experiments, G. Snook for SEM images and CSIRO division of Minerals for use of the scanning electron microscope.

## References

1 See for example: E. Papaconstantinou, *Chem. Soc. Rev.*, 1989, **18**, 1; M. T. Pope and A. Müller, in *Polyoxometalates: From Platonic Solids To Anti-Retroviral Activity*, Kluwer Academic Publishers, Dordrecht, 1994; C. L. Hill and C. M. Prosser-McCartha, *Coord. Chem. Rev.*, 1995, **143**, 407; R. Neumann, *Prog. Inorg. Chem.*, 1998, **47**, 317; C. L. Hill, *J. Mol. Catal.*, 1996, **114**, 1.
2 M. Sadakane and E. Steckhan, *Chem. Rev.*, 1998, **98**, 219; B. Keita, L. Nadjo, G. Krier and J. F. Muller, *J. Electroanal. Chem. Interfacial Electrochem.*, 1987, **223**, 287; B. Keita and L. Nadjo, *J. Electroanal. Chem. Interfacial Electrochem.*, 1988, **243**, 87; Keita, B. and L. Nadjo, *J. Electroanal. Chem. Interfacial Electrochem.*, 1987, **227**, 265; A. Kuhn, N. Mano and C. Vidal, *J. Electroanal. Chem. Interfacial Electrochem.*, 1999, **462**, 187; D. Ingersoll, P. J. Kulesza and L. R. Faulkner, *J. Electrochem. Soc.*, 1994, **141**, 140; P. J. Kulesza, G. Roslonek and L. R. Faulkner, *J. Electroanal. Chem. Interfacial Electrochem.*, 1990, **280**, 233.
3 A. Kuhn and F. C. Anson, *Langmuir*, 1996, **12**, 5481.
4 S. Himeno, T. Osakai, A. Saito, K. Maeda and T. Hori, *J. Electroanal. Chem. Interfacial Electrochem.*, 1992, **337**, 371; S. Himeno, K. Maeda, T. Osaki, A. Saito and T. Hori, *Bull. Chem. Soc. Jpn.*, 1993, **66**, 109.
5 D. M. Way, A. M. Bond and A. G. Wedd, *Inorg. Chem.*, 1997, **36**, 2826.
6 D. M. Way, J. B. Cooper, M. Sadek, T. Vu, P. J. Mahon, A. M. Bond, R. T. C. Brownlee and A. G. Wedd, *Inorg. Chem.*, 1997, **36**, 4227.
7 J. E. Huheey, *Inorganic Chemistry*, 3rd edn., Harper International, Cambridge, 1983, p. 340.
8 C. M. Elliot and E. J. Hershenhart, *J. Am. Chem. Soc.*, 1982, **104**, 7519; A. Juris, V. Balzani, F. Barigelletti, S. Campagna, P. Beiser and A. von Zelewsky, *Coord. Chem. Rev.*, 1988, **84**, 85.
9 R. J. Forster, T. E. Keyes and A. M. Bond, *J. Phys. Chem. B*, 2000, **104**, 6389.
10 M. E. G. Lyons, in *Electroactive Polymer Electrochemistry*, Plenum Press, New York, 1999.
11 P. T. Kissinger and W. R. Heineman, in *Laboratory Techniques in Electroanalytical Chemistry*, Second Edition, Marcel Dekker, New York, 1996, p. 481.
12 J. B. Cooper, D. M. Way, A. M. Bond and A. G. Wedd, *Inorg. Chem.*, 1993, **32**, 2416.
13 A. M. Bond, M. Fleischmann and J. Robinson, *J. Electroanal Chem. Interfacial Chem.*, 1984, **168**, 299.
14 A. M. Bond, D. M. Way, A. G. Wedd, R. G. Compton, J. Booth and J. C. Eklund, *Inorg. Chem.*, 1995, **34**, 3378.